



SEISMIC RETROFIT AND REPAIR OF REINFORCED CONCRETE BRIDGE WALL PIERS

C.P. Pantelides⁽¹⁾, B. Kunwar⁽²⁾, V. McEntee⁽³⁾

⁽¹⁾ Professor, Dept. Civil and Environmental Engineering, University of Utah, Salt Lake City, UT, USA, c.pantelides@utah.edu

⁽²⁾ Res. Asst., Dept. Civil and Environmental Engineering, University of Utah, Salt Lake City, UT, USA, kunwar5bhaskar@gmail.com

⁽³⁾ Res. Asst., Dept. Civil and Environmental Engineering, University of Utah, Salt Lake City, UT, USA, vanessa.mcentee@gmail.com

Abstract

Reinforced concrete bridge wall piers constructed using older codes perform inadequately during strong earthquakes; deficiencies include short reinforcement lap splices, insufficient steel reinforcement ratios in the longitudinal and transverse direction, and inadequate seismic detailing. Three half-scale wall piers were constructed using as-built reinforcement details conforming to older bridge codes; an identical fourth specimen was constructed using current seismic code-compliant reinforcement details. A total of six quasi-static cyclic tests were conducted about the weak axis of the wall piers: (i) first as-built pier; (ii) code-compliant pier; (iii) retrofit of second as-built pier using near surface mounted (NSM) carbon fiber reinforced polymer (CFRP) rods, horizontal CFRP anchors and CFRP jackets; (iv) retrofit of third as-built pier using vertical and horizontal CFRP anchors and CFRP jackets; (v) repair of first as-built pier using mild steel NSM bars, horizontal CFRP anchors and CFRP jackets; and (vi) repair of code-compliant pier using a CFRP shell with vertical headed steel bars for relocating the plastic hinge. The two retrofit methods increased the initial stiffness of the as-built pier by 110%, the load carrying capacity by 73%, and the hysteretic energy dissipation capacity by 67%. The repair method of the as-built pier increased the initial stiffness of the as-built pier by 50%, load carrying capacity by 73% with similar hysteretic energy dissipation. The repair method of the code-compliant pier increased the initial stiffness by 31%, load carrying capacity by 15%, and hysteretic energy capacity by 55% for lateral displacements that reached a 6% drift ratio.

Keywords: concrete; FRP; pier; repair; retrofit.



1. Introduction

Many bridges constructed using before the 1970s exhibit inadequate lap splices and transverse reinforcement; this results in weak confinement and insufficient clamping action in the lap splice region to prevent debonding [1, 2]. During large earthquakes, the increased drift demand and steel stress reversals cause bond splitting of the lap spliced longitudinal bars. This bond failure causes flexural and stiffness degradation of the wall pier. Studies following large earthquakes such as Loma Prieta (1989), Northridge (1994), and Kobe (1995) validate this lap splice failure [3]. In order to improve the performance of these deficient bridge wall piers in a strong earthquake, a seismic retrofit is required.

External confinement is the most common way to increase the bond strength of the lap spliced longitudinal reinforcement. Current retrofit methods to address confinement issues include steel and carbon fiber reinforced polymer jackets. Most of this research focuses on columns, and little has been studied on jacketing of bridge wall piers. CFRP jacketing, however, does not typically extend beyond the existing member into the joint and it will not increase the flexural resistance and stiffness of the member, but will improve shear strength, deformation capacity and splicing of longitudinal reinforcement [4]. To increase the flexural resistance of a member current retrofit methods include using CFRP vertical anchors [5, 6] or near-surface mounted (NSM) bars [7] in conjunction with CFRP jacketing. These techniques involve the placement of reinforcement in epoxy filled pre-cut grooves (for NSM) or pre-drilled holes (for CFRP vertical anchors) into the footing.

Recent research on the use of NSM bars and CFRP jacketing shows a significant increase in the flexural capacity [4, 8, 9]. In addition to CFRP jacketing for confinement and vertical anchorage for flexural strengthening, research has shown that the use of horizontal CFRP anchors in conjunction with these methods offers increased confinement, bond strength, shear capacity and strengthening [10, 11, 12]. There have been a few studies on the repair of severely damaged concrete wall piers. A plastic hinge relocation technique was developed to repair severely damaged reinforced concrete columns by the relocation of the plastic hinge to a position slightly higher in the column that remained elastic during the initial test. A combination of Carbon Fiber Reinforced Polymer (CFRP) wraps and CFRP vertical anchors was one of the methods used for relocating the plastic hinge [13] or CFRP wraps with vertical headed steel bars [14, 15]. FRP confinement is more effective for confining circular sections as compared to rectangular or square cross-sections. One approach of strengthening rectangular or square columns using FRP confinement is to perform a shape modification of the cross-section into elliptical, oval, or circular section [16].

2. Control Wall Piers

The research used wall pier specimens with a 1:2 scale of an actual wall pier. The replicated wall dimensions were 2.74 m x 1.22 m x 0.30 m and the footing dimensions were 1.83 m x 1.52 m x 0.46 m. Three wall piers were built in the as-built condition representing existing piers designed to old codes not conforming to current seismic standards, and one wall pier was built with modern code-conforming details. All wall piers were built with concrete having a compressive strength of 35 MPa on the day of testing. Mild reinforcing steel was used with an average yield stress equal to 448 MPa and ultimate strength of 710 MPa. An axial load of 534 kN was applied at the top of all wall piers corresponding to 6% of the ultimate axial load carrying capacity.

2.1 As-built wall pier

The three as-built wall piers had two curtains of 10 mm vertical steel rebar spaced at 190 mm on each face, as well as 10 mm transverse steel spaced at 229 mm on center. The footing was comprised of 16 mm bars spaced at 152 mm on the top and bottom, confined with 17 double stirrups having a 10 mm diameter both externally and internally located. The lap splices consisted of 14 bars with a 10 mm diameter with a 635 mm length and extending 356 mm, or 37 bar diameters above the footing; these lap splices were the only



connection between the wall pier and footing. The dimensions of the as-built wall pier and reinforcement details can be seen in Fig. 1(a). The as-built wall piers do not meet the AASHTO [17] seismic design criteria for steel detailing in the longitudinal or transverse direction, most notably that there is a lap splice of longitudinal steel in the plastic hinge region. The wall piers were tested under quasi-static loading about the weak axis using the test setup shown in Fig. 1(b); the load was applied 2.44 m above the top of the footing.

The hysteresis for the control as-built wall pier can be seen in Fig. 2(a) where pinching is evident; lap splice failure developed gradually until the first cycle of the 6.0% drift ratio when a significant drop in lateral load was observed. The strain in the lap spliced bars is shown in Fig. 2(b); the lap splices did not develop the yield strain during the test, but actually the lap spliced bars in the wall reached the yield point. Moreover, the difference in strain between footing bars and bars in the wall pier is greater than 1000 microstrains, which indicates lap splice failure had occurred. At 2.0% drift ratio, cracks began to widen on both sides of the wall pier measuring 0.33 mm. During the 3.0% drift ratio, the plastic hinge had formed completely and cracks grew to a width of 0.76 mm. The lateral load began decreasing at the 4.0% drift ratio with significant damage shown in Fig. 3; at the 6.0% drift ratio the wall failed due to loss of the lap splice tension capacity. The as-built wall pier behaved poorly, hysteretic energy dissipation was low and the lateral load degraded significantly; the as-built wall pier would have performed poorly in a strong earthquake.

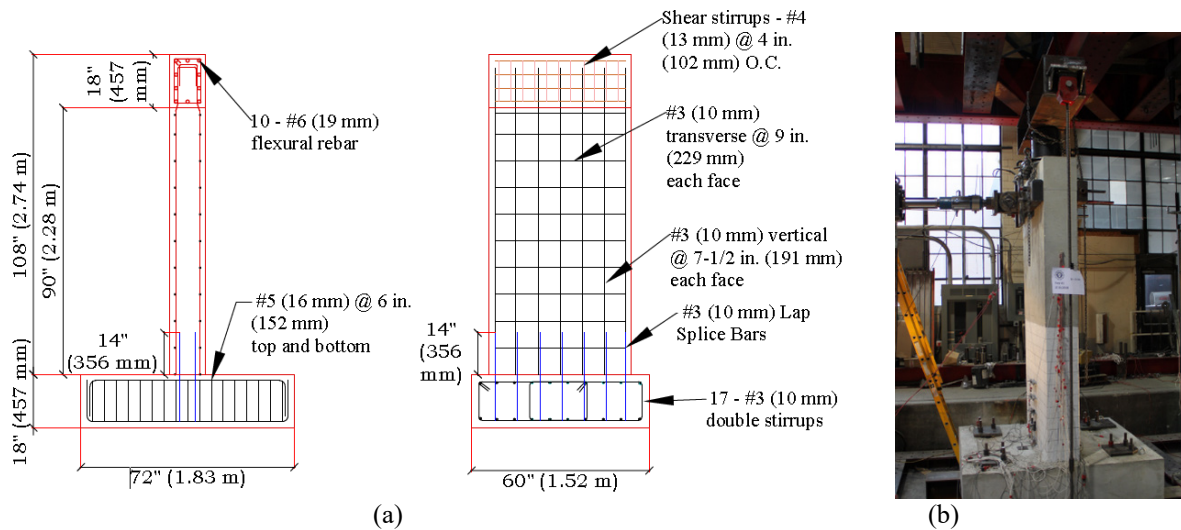


Fig. 1 – Concrete wall pier: (a) as-built wall pier details and reinforcement; (b) test setup

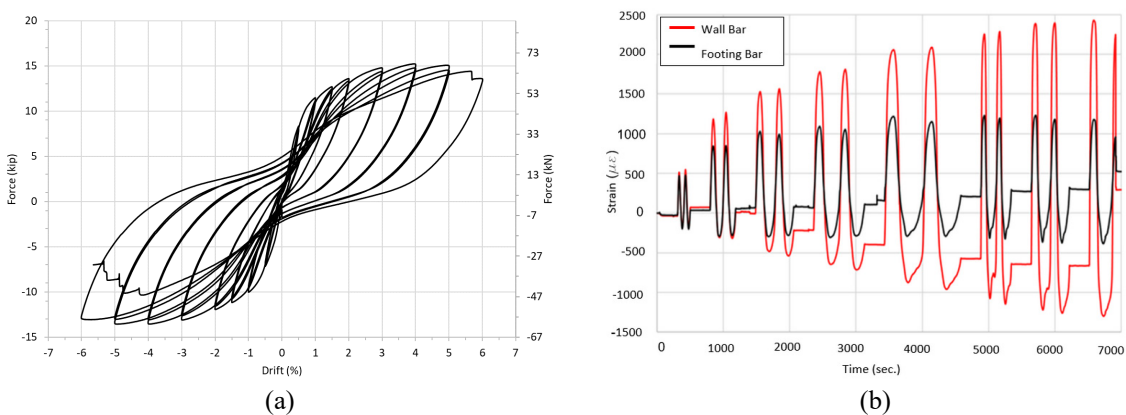


Fig. 2 – Performance of as-built wall pier: (a) hysteresis; (b) lap-splice wall and footing bar strains



Fig. 3 – As-built wall pier spalling occurring at 4.0% drift ratio

2.2 Code-compliant pier

The geometry of the code-compliant pier was identical to the as-built wall pier but the reinforcement complied to AASHTO [17] seismic design criteria. Fourteen steel bars 19 mm in diameter were placed in the longitudinal direction with seven bars on each face. In addition, 13 mm transverse hoops were provided at a 102 mm spacing in the plastic hinge region and a 229 mm spacing for the remaining height. The longitudinal and transverse reinforcement ratio was 1.07% and 1.7%, respectively. Outside the plastic hinge region, the transverse reinforcement ratio was 1.07%, which is still higher than 1.0% as required by AASHTO [17]. The reinforcement layout of the current code-compliant specimen can be seen in Fig. 4. All major cracks developed during the 6.0% drift ratio. The wall pier began to respond differently in the two directions as more damage was observed in the west direction. The cracks increased to 1.0 mm in the west direction while in the east direction their size reached 0.8 mm. During the 7.0% drift ratio, spalling started in the east direction, whereas new diagonal cracks were observed in the west direction. Concrete spalling progressed over the wall height up to 610 mm, with more spalling over the sides of the wall at the 8.0% drift ratio. During the 9.0% drift ratio, spalling was severe and was transmitted to the inner part of the wall. The major flexural cracks were joined over the periphery of the wall. In the first cycle of the 10.0% drift ratio, a slight drop in strength was observed and in the second cycle of the 10.0% drift ratio, one of the bars on the west face fractured 100 mm above the top of the footing. The severely spalled region was restricted to 300 mm in the west and 150 mm in the east direction. Major structural cracks extended for a height of 560 mm above the top of the footing. The code-compliant wall pier dissipated 5.7 times the hysteretic energy and reached 2.1 times the lateral load of the as-built wall pier and had a ductile failure.

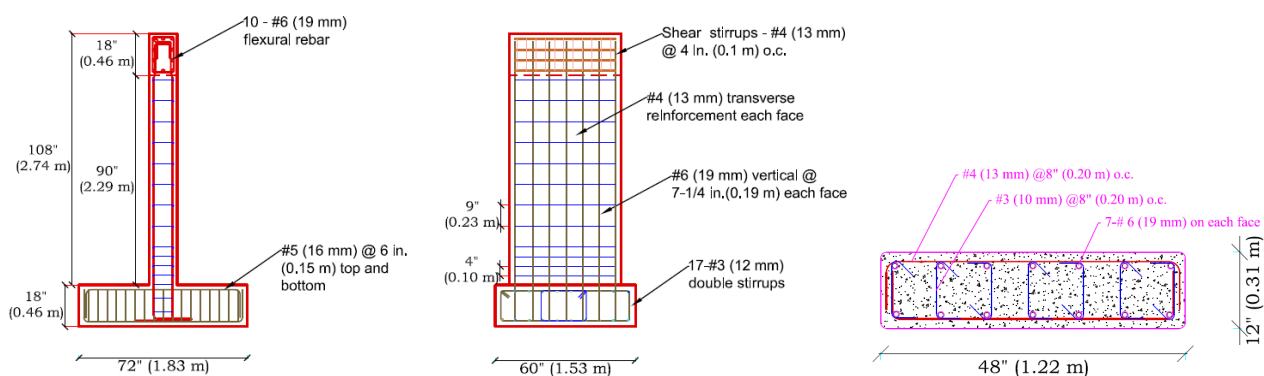


Fig. 4 – Reinforcement details of current code-compliant wall pier

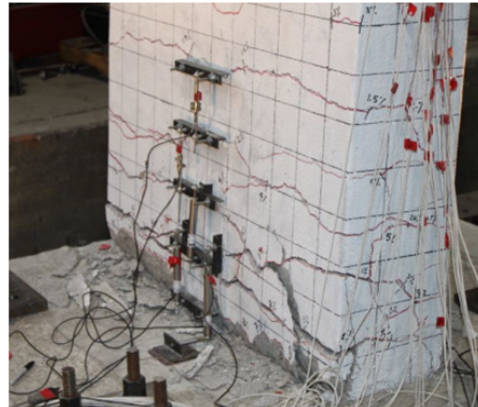
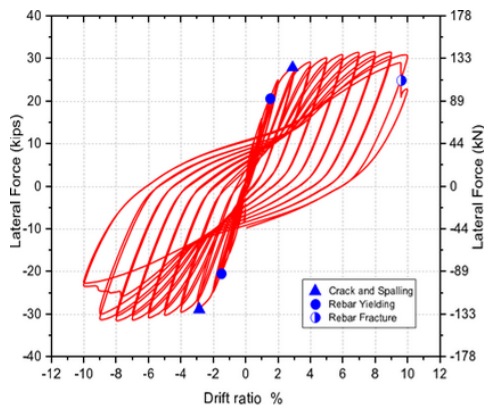


Fig. 5 – Hysteresis and damage state at 10% drift ratio of code compliant wall pier with rebar fracture

3. Retrofitted Wall Piers

The remaining two as-built wall piers were retrofitted using a combination of CFRP systems before testing. The two specimens were built and tested as specified in Section 2. The retrofit aimed at improving the seismic performance of the wall pier so that it could achieve code compliance and dissipate significant hysteretic energy. CFRP jackets, sheets and wraps were used with the following properties: tensile strength = 1240 MPa, modulus of elasticity = 74 GPa, elongation = 1.7%, and layer thickness = 1.0 mm. Horizontal CFRP anchors used had the following properties: tensile strength = 834 MPa, modulus of elasticity = 82 GPa, and elongation = 0.85%.

3.1 Retrofit of as-built pier using vertical and horizontal CFRP anchors and CFRP jackets

The retrofit was designed using nine 16 mm diameter vertical CFRP anchors on each side of the wall that were embedded into the footing 305 mm and extended 457 mm up the face of the wall, above the footing, as shown in Fig. 6(a). The vertical CFRP anchors were used to create a positive connection between the footing and wall pier under the assumption of failure of the steel lap splices. The properties of the vertical CFRP anchors were: tensile strength = 1241 MPa, modulus of elasticity = 98 GPa, and elongation = 1.17%. There were also two layers of vertically oriented CFRP sheets which were applied first to the wall for flexural strengthening, as shown in Fig. 6(a). Ten 18 mm diameter horizontal CFRP anchors were placed through the wall thickness to add confinement and shear friction capacity to the lap spliced region of the wall pier, as shown in Fig. 6(b). The CFRP anchors and vertical layers were confined with unidirectional CFRP wraps in the hoop direction. These included three layers of 610 mm high segments at the base, two layers of 305 mm segments above that, and one layer of another 1.22 m high segments above that, as shown in Fig. 6(c).

The hysteresis in Fig. 7(a) exhibited general stability throughout the entire test until the first cycle of 5.0% drift at which the maximum force dropped by 34%. A comparison between the footing bar strain and the wall bar strain in Fig. 7(b) shows the reduction in lap splice strain from the addition of the CFRP retrofit compared to Fig. 2(b) of the as-built wall pier. In the as-built wall pier test, the lap splices were increasingly strained throughout the test, reaching up to 1200 microstrain at 5.0% drift ratio. However, in the retrofit specimen, the lap splice strain ceased increasing after the 2.0% drift ratio and was at a maximum of 830 microstrain at this drift ratio. There was not a large difference in strain between footing bars and wall bars; in addition, none of the spliced bars yielded which implies that there was no lap splice failure. During the first cycle of the 2.0% drift ratio, two vertical CFRP anchors partially fractured on the west side of the wall, as shown in Fig. 8. At the 3.0% drift ratio, a 6.4 mm wide crack opened up on the east face of the wall and portions of the concrete began to spall at the base of the footing. After the 3.0% ratio there was no more debonding of the CFRP, and damage for the remainder of the test occurred in the footing. At 4.0% drift ratio the footing crack increased to 25 mm and at the 5.0% drift ratio, during the pull cycle, the lateral load dropped when two vertical anchors fractured, and steel rebar was exposed in the footing due to concrete



spalling. The retrofit specimen performed better than the as-built, although it lost 20% of its lateral load resistance after the 2.0% drift ratio. Hysteretic energy dissipation was 1.6 times that of the as-built wall pier, and reached 1.8 times the lateral load of the as-built wall pier.

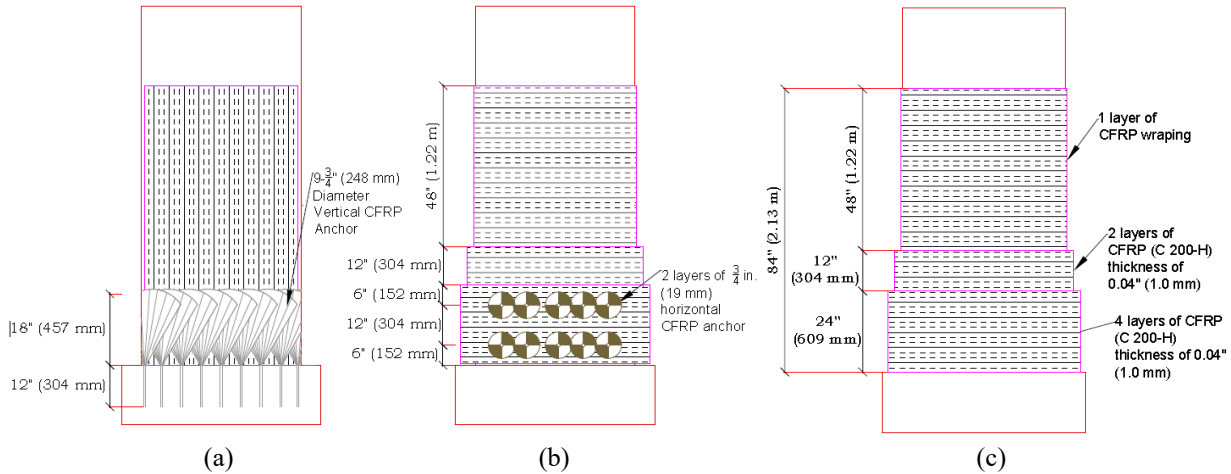


Fig. 6 – Retrofit design; (a) vertical CFRP sheet and CFRP anchors, (b) horizontal CFRP anchors, (c) hoop direction CFRP wraps

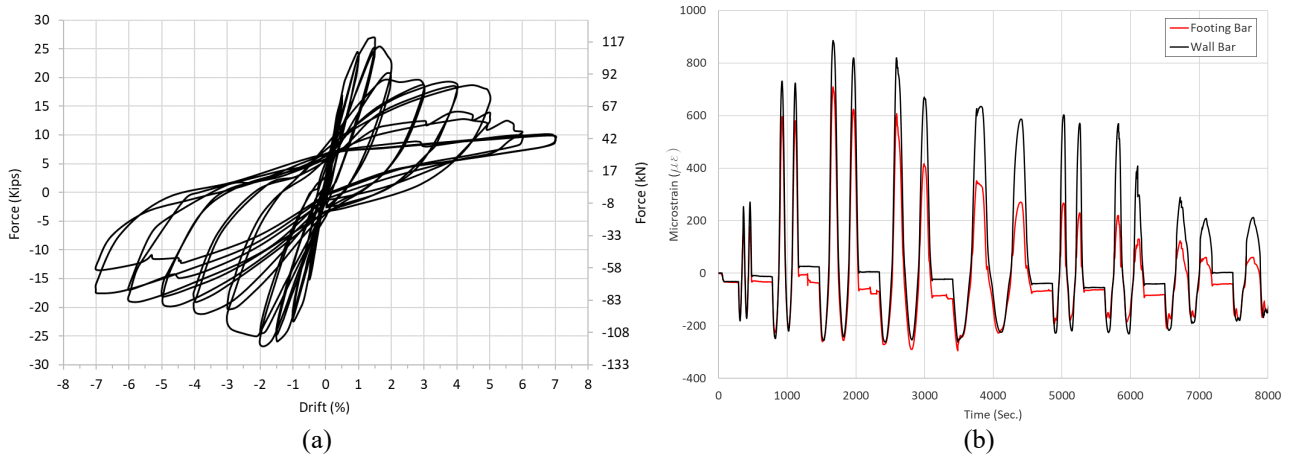


Fig. 7 – Performance of retrofitted wall pier with vertical CFRP anchors: (a) hysteresis; (b) lap-splice wall and footing bar strains



Fig. 8 – Partial anchor fracture for retrofitted wall pier with vertical CFRP anchors



3.2 Retrofit of as-built pier using NSM CFRP rods, horizontal CFRP anchors and CFRP jackets

To provide flexural strength and a smooth transition of applied lateral force from the wall to the footing, CFRP NSM rods were provided as shown in Fig. 9(a). Nine 13 mm CFRP NSM rods were provided on each face of the wall pier for a total of 18 rods; the CFRP rod properties were as follows: tensile strength = 2068 MPa, modulus of elasticity = 131 GPa and elongation = 1.58%. A square groove of a dimension 19mm by 19mm which is at least 1.5 times the diameter of the CFRP rod was provided. In order to prevent pullout failure and to develop a high effective tensile stress at a given section, a 381mm or $32d_b$ anchorage length was provided for the CFRP NSM rods. In the lap spliced region of the longitudinal steel bars, CFRP horizontal anchors provide confinement and shear friction capacity to avoid bond-splitting failure. Using the shear friction principle, ten 18 mm diameter CFRP horizontal anchors were provided as shown in Fig. 9(b). To provide shear strength and confinement in the plastic hinge region, CFRP wraps in the hoop direction were provided. Four layers of 610 mm segments at the base, two layers of 305 mm segments above that, and one layer for another 1.22 m above that were provided as shown in Fig. 9(c).

The hysteresis curve in Fig. 10(a) shows that the specimen continues to resist lateral force until the 1.5% drift ratio where a sharp loss in the lateral load-carrying capacity is observed in the push direction. Premature debonding failure of two NSM CFRP rods was observed, resulting in significant loss of lateral load-carrying capacity of the specimen. Fig. 11 shows the premature bond failure of one of the CFRP bars. The retrofitted specimen had enough strength to resist the applied lateral force in the pull direction. This premature bond failure at 1.5 % drift ratio, resulted in the eventual failure of the specimen at a 5.0% drift ratio, at which point the lateral force dropped by 19.5%. The starter bars in the footing had a maximum strain of 1000 microstrain, whereas the strain of the main bars in the wall pier at the same height was 2500 microstrain and thus they yielded, as shown in Fig. 10(b). The CFRP NSM rods transferred the tensile force generated through the applied lateral force to the footing. According to strain gauge data, the CFRP NSM rods reached a maximum 0.50% strain in tension and 0.34% strain in compression, which is 32% of ultimate tensile strain capacity. In general, the CFRP NSM fiber rod do not take any compressive forces; however, in a retrofit, the CFRP NSM rods were jacketed with four layers of CFRP sheets, which enabled them to take some compressive force. At a 2.0% drift ratio, the cracks on top of the footing joined to form a continuous loop around the wall. A new prominent crack was seen on the side of the footing at a 3.0% drift ratio. The size of the crack on top of the footing increased to 0.13 mm in width at a 4.0% drift ratio. The lateral load capacity of the specimen started to degrade at the 5.0% drift ratio when the cracks in the footing were greater than 5mm wide. The test was terminated at the 7.0% drift ratio, since the lateral load capacity of the specimen was only half of the maximum load capacity. Hysteretic energy dissipation was 1.7 times that of the as-built wall pier; the retrofitted wall pier reached 1.6 times the lateral load of the as-built wall pier and overall it performed better than the as-built wall pier.

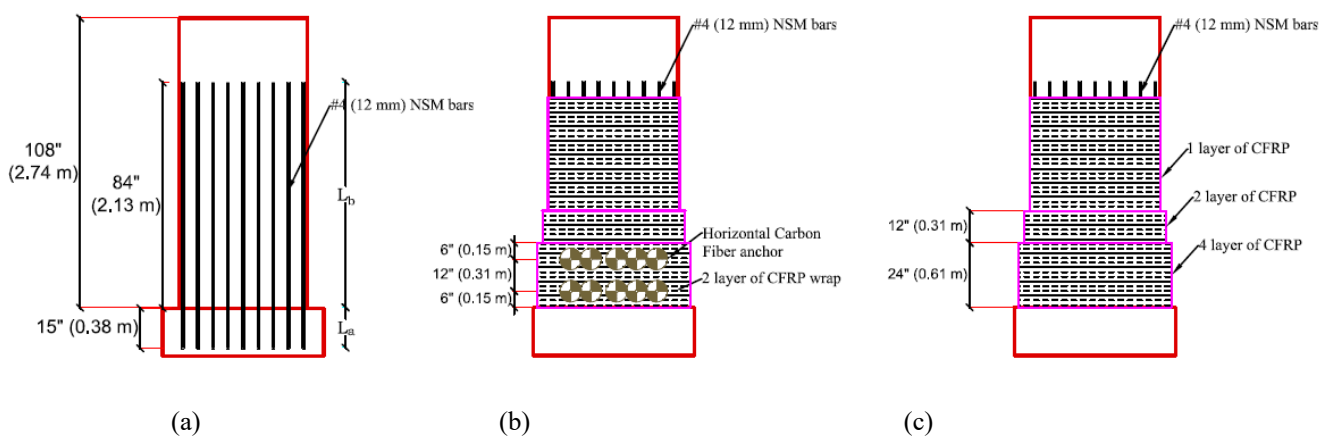


Fig. 9 – Retrofit design; (a) NSM CFRP rods, (b) horizontal CFRP anchors, (c) hoop direction CFRP wraps

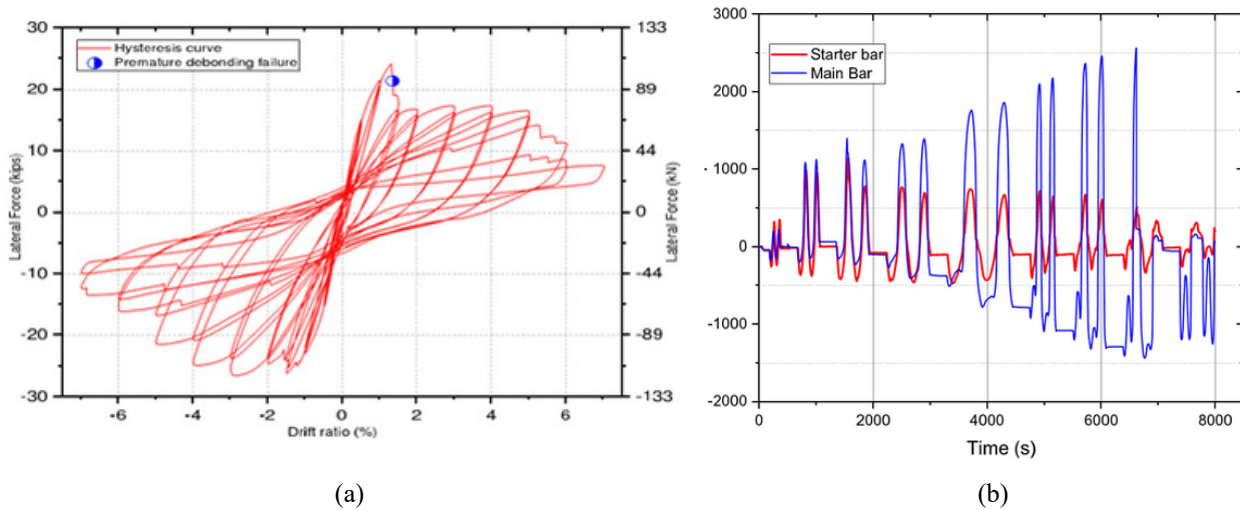


Fig. 10 – Performance of retrofitted wall pier with NSM CFRP rods: (a) hysteresis; (b) lap-splice wall and footing bar strains

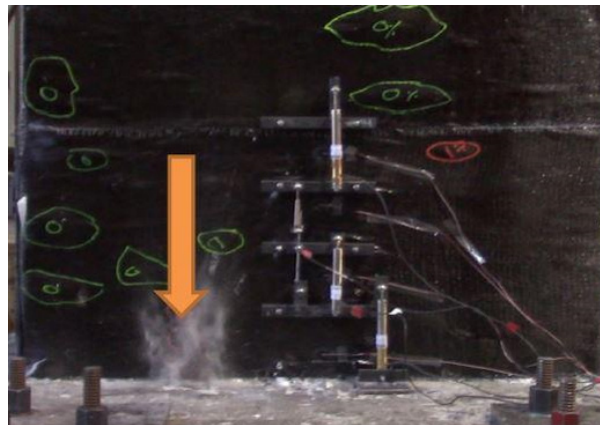


Fig. 11 – Bond Failure of CFRP NSM rods

4. Repaired Wall Piers

The as-built control pier was repaired after initial testing as described in Section 2.1. In addition, the code-compliant pier was repaired after initial testing as described in Section 2.2.

4.1 Repair of as-built pier using mild steel NSM bars, horizontal CFRP anchors and CFRP jackets

The repair included the use of both mild steel NSM bars, CFRP wraps in the hoop direction and CFRP horizontal anchors through the wall thickness. The repair aimed at bringing the wall pier back to a safe condition. The repair was designed using seven 1.68 m long 13 mm mild steel rebar embedded in vertical grooves 19 mm into the wall on both sides, for a total of fourteen steel bars as shown in Fig. 12(a). These were confined with CFRP wraps oriented in the hoop direction; they included four layers of 610 mm segments at the base, two layers of 305 mm segments above that, and one layer for another 610 mm above that as shown in Fig. 12(c). After the first two CFRP layers were placed in the hoop direction at the base of the wall, ten 18 mm diameter CFRP horizontal anchors were placed through the wall thickness to add confinement to the lap spliced region of the pier and increase the normal pressure to improve the shear friction capacity of the lap splice as shown in Fig. 12(b). These CFRP anchors were then confined by two



additional layers of CFRP wraps in the hoop direction as shown in Fig. 12(c). The hysteresis in Fig. 13 exhibited general stability throughout the test until the first cycle of the 5.0% drift ratio, in which the lateral load dropped 34% from the peak load.

There was no visible cracking exhibited in the wall pier or footing until the 1.5% drift ratio. At this point, hairline cracks were observed in the footing and at the interface of the wall and footing. At 2.0% drift ratio, the cracks at the interface of the wall and footing spread around the entire base of the wall. No debonding occurred on the CFRP wrap surface until the 3.0% drift ratio. These debonded regions began to form at the base of the footing on the east wall face, the majority of which were located at segments of the mild steel NSM bars underneath the CFRP jacket. After the 4.0% drift cycle, there was a 36% drop in pull and a 63% drop in push; the test was terminated at the 5% drift ratio as shown in Fig. 13. The pier failed in the second cycle of the 4.0% drift ratio due to debonding of the mild steel NSM bars. The cumulative hysteretic energy dissipation was 90% that of the as-built wall pier, however, the repaired wall had a larger cumulative energy dissipation until the end of the 3.0% drift ratio. The repaired wall pier reached the 4.0% drift ratio with a lateral load 1.4 times the lateral load of the as-built wall pier.

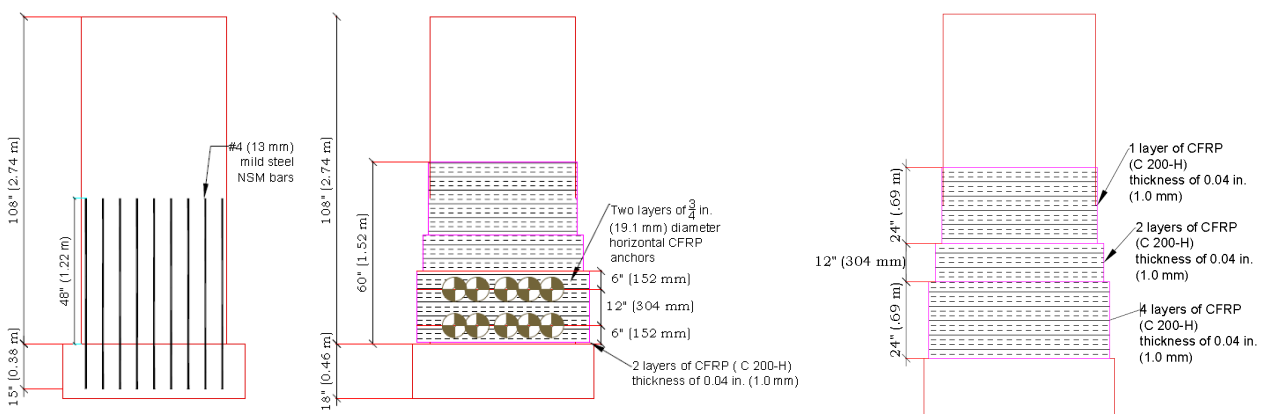


Fig. 12 – Repair of as-built pier: (a) steel NSM bars (b) horizontal CFRP anchors, (c) hoop direction CFRP wraps

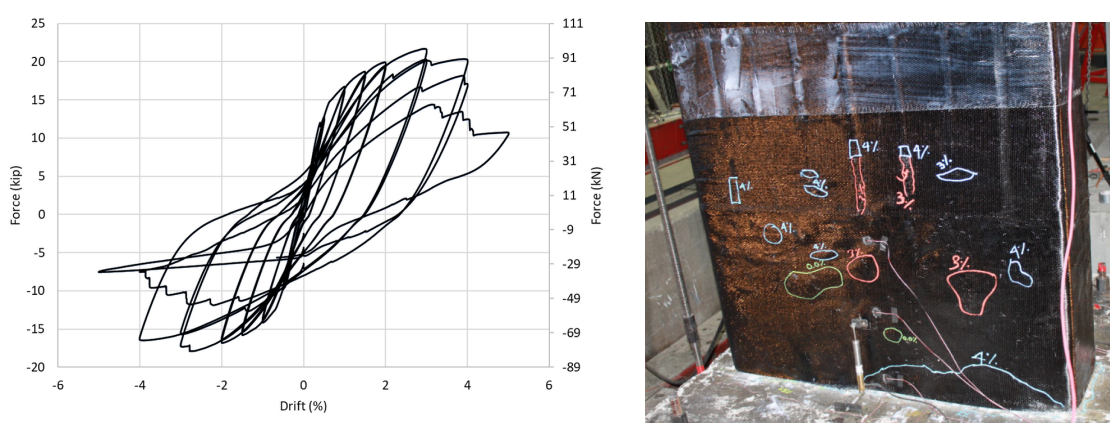


Fig. 13 – Hysteresis and CFRP wrap debonding areas at 5.0% drift ratio for repaired as-built wall pier

4.2 Repair of code-compliant pier using a CFRP shell with vertical headed mild steel bars

The damaged code-compliant wall pier of Section 2.2 was repaired to restore both its stiffness and load-carrying capacity. The specimen was repaired using the plastic hinge relocation technique. The primary objective of this technique is to strengthen the original damaged region to withstand additional shear and



bending moment that would be generated in a future earthquake. To move the plastic hinge to a new location, the damaged section of the wall pier was enlarged to an elliptical shape using a prefabricated CFRP shell. All cracks were sealed using a sealant. The injection points were installed along the cracks with the sealant at a 127 mm spacing. Epoxy was injected from all entry points, starting from the bottom. The modified wall section consisted of epoxy anchored headed steel bars with the void filled between the wall pier and shell with expansive cement concrete. The CFRP shell provided confinement and acted as formwork for the additional cast concrete. The rectangular cross-section of the wall pier at the repaired region was converted to an elliptical section with a 762 mm minor axis and 1524 mm major axis with a height of 610 mm, as shown in Fig. 14. Six 16 mm headed steel bars embedded 343 mm in the footing were provided on each face of the concrete wall pier to reestablish the flexural strength and tension transfer between the wall pier and footing as shown in Fig. 14. No shrink concrete with a compressive strength of 28 MPa was provided in the CFRP shell. To increase the bond between the wall pier concrete and expansive cement concrete, a steel collar consisting of steel plates and steel studs was installed on the wall perimeter inside the CFRP shell. The steel plate used for the collar was 10 mm thick and 152 mm high. Nine layers of CFRP jacket were provided to improve confinement, shear capacity and act as formwork for the repaired elliptical shape as shown in Fig. 14. In addition, one vertical CFRP layer was provided to prevent cracking and splitting of the fibers in the hoop direction.

The repair system performed well in relocating the plastic hinge. No failure was observed in the repair system. The CFRP shell was intact and did not experience any cracking until the end of the experiment. The lateral load capacity of the repaired pier reached 13% higher than the original code-compliant wall pier before failure, as shown in Fig. 14. Hysteresis loops were symmetric, wide and stable without major strength degradation. The test ended at the end of the 6% drift ratio with a 37 % drop in lateral force capacity of the specimen due to buckling of the vertical bars above the repair, as shown in Fig. 14. The repair method was applied successfully and restored both the load-carrying capacity as well as stiffness of a damaged reinforced concrete wall pier with a cross-section aspect ratio of four.

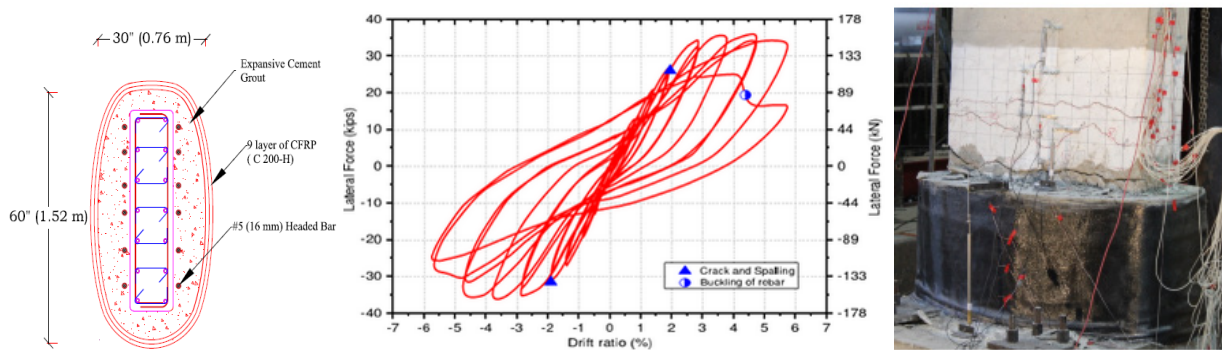


Fig. 14 – Elliptical cross-section, hysteresis and damage at 6% drift ratio of repaired code compliant pier

5. Conclusions

The aim of this research is to determine and compare the performance of an as-built wall pier with deficient seismic details to a current seismic code compliant wall pier. In addition, retrofit and repair methods are developed to mitigate seismic deficiencies either before or after a seismic event. The as-built wall pier specimen had seismic deficiencies including inadequate length and confinement of lap splices of longitudinal reinforcement in the plastic hinge region, inadequate longitudinal and transverse steel reinforcement, and a lack of seismic detailing. The as-built wall pier behaviour was substandard, hysteretic energy dissipation was low and the lateral load degraded significantly; the as-built wall pier would have performed poorly in a strong earthquake. The code-compliant wall pier designed with modern seismic details performed very well in a ductile manner reaching a 10.0% drift ratio, with one of the bars fracturing above the top of the footing; it dissipated 5.7 times the hysteretic energy and reached 2.1 times the lateral load capacity of the as-built



wall pier and had a ductile failure. Two as-built wall piers were retrofitted using either vertical CFRP anchors or NSM CFRP rods. Both retrofits were effective in postponing failure of the lap-spliced bars. The first retrofit with vertical and horizontal CFRP anchors and CFRP jackets showed better performance than the as-built pier, although it lost 20% of its lateral load capacity because of fracture of two vertical CFRP anchors; its hysteretic energy dissipation was 1.6 times that of the as-built wall pier, and it reached 1.8 times the lateral load of the as-built wall pier. The second retrofit was implemented using NSM CFRP rods, horizontal CFRP anchors and CFRP jackets; the retrofitted pier lost its capacity due to debonding failure of two NSM CFRP rods; its hysteretic energy dissipation was 1.7 times that of the as-built wall pier, and it reached 1.6 times the lateral load of the as-built wall pier and performed better than the as-built pier. After the initial test, the as-built control pier was repaired using mild steel NSM bars, horizontal CFRP anchors and CFRP jackets; the repaired as-built pier failed in the second cycle of the 4.0% drift ratio due to debonding of the mild steel NSM bars; it reached the 4.0% drift ratio with a lateral load 1.4 times the lateral load of the as-built wall pier; cumulative hysteretic energy dissipation was 90% that of the as-built wall pier, but it had a larger cumulative energy dissipation until the end of the 3.0% drift ratio. The code-compliant pier was also repaired after initial testing using headed mild steel bars and a CFRP shell; the lateral load capacity of the repaired pier was 13% higher than the original code-compliant wall pier, hysteresis loops were symmetric and stable without major strength degradation. The test ended at the 6% drift ratio due to buckling of the vertical bars above the repair. The repair method was successful and it restored both the load-carrying capacity as well as the stiffness of a damaged code-compliant wall pier with a cross-section aspect ratio of four.

5. Acknowledgements

The authors acknowledge the financial support provided by the Mountain-Plains Consortium (MPC) under project MPC-526. In addition, they acknowledge the support of Structural Technologies, and the assistance of Dr. Tarek Alkhradji.

6. References

- [1] Elsanadedy HM, Haroun MA (2005): Seismic design criteria for circular lap spliced reinforced concrete bridge columns retrofitted with fiber-reinforced polymer jackets. *ACI Structural Journal*, **102** (3), 354-362.
- [2] Pantelides CP, Alameddine F, Sardo T, Imbsen R (2004): Seismic retrofit of State Street Bridge on Interstate 80. *Journal of Bridge Engineering*, **9** (4), 333-342.
- [3] Priestley MJ, Seible F, Calvi GM (1996): *Seismic Design and Retrofit of Bridges*. Wiley 1st edition.
- [4] Bousias S, Spathis AL, Fardis MN (2007): Seismic retrofitting of columns with lap spliced smooth bars through FRP or concrete jackets. *Journal of Earthquake Engineering*, **11** (5), 653-674.
- [5] Vrettos I, Kefala E, Triantafillou TC (2013): Innovative flexural strengthening of reinforced concrete columns using carbon-fiber anchors. *ACI Structural Journal*, **110** (1), 63-70.
- [6] Bournas DA, Pavese A, Tizani W (2015): Tensile capacity of FRP anchors in connecting FRP and TRM sheets to concrete. *Engineering Structures*, **82**, 72-81.
- [7] Bournas DA, Triantafillou TC (2009): Flexural strengthening of reinforced concrete columns with near-surface-mounted FRP or stainless steel. *ACI Structural Journal*, **106** (4), 495-505.
- [8] Jiang SF, Zeng X, Shen S, Xu X (2016): Experimental studies on the seismic behavior of earthquake-damaged circular bridge columns repaired by using combination of near-surface-mounted BFRP bars with external BFRP sheets jacketing. *Engineering Structures*, **106**, 317-331.
- [9] Seifi A, Hosseini A, Marefat MS, Khanmohammadi M (2018): Seismic retrofitting of old-type RC columns with different lap splices by NSM GFRP and steel bars. *Structural Design of Tall and Special Buildings*, **27** (2), 1-21.
- [10] Perrone M, Barros JAO, Aprile A (2009): CFRP-based strengthening technique to increase the flexural and energy dissipation capacities of RC columns. *Journal of Composites for Construction*, **13** (5), 372-383.



- [11] Kim IS, Jirsa JO, Bayrak O (2011): Use of carbon fiber-reinforced polymer anchors to repair and strengthen lap splices of reinforced concrete columns. *ACI Structural Journal*, **108** (5), 630–640.
- [12] Nye TK, Pantelides CP, Alkhradji T (2018): Bidirectional GFRP-composite connections between precast concrete wall panels under simulated seismic load. *Journal of Composites for Construction*, **22** (4), 1–13.
- [13] Rutledge ST, Kowalsky MJ, Seracino R, Nau JM (2014): Repair of reinforced concrete bridge columns containing buckled and fractured reinforcement by plastic hinge relocation. *Journal of Bridge Engineering*, **19** (8), A4013001.183
- [14] Parks JE, Brown DN, Ameli MJ, Pantelides CP (2016): Seismic repair of severely damaged precast reinforced concrete bridge columns connected with grouted splice sleeves. *ACI Structural Journal*, **113** (3), 615–626.
- [15] Wu RY, Pantelides CP (2017): Rapid seismic repair of reinforced concrete bridge columns. *ACI Structural Journal*, **114** (5), 1339–1350.
- [16] Yan Z, Pantelides CP (2011): Concrete column shape modification with FRP shells and expansive cement concrete. *Construction and Building Materials*, **25** (1), 396–405.
- [17] AASHTO (2011): *AASHTO Guide Specifications for LRFD Seismic Bridge Design*. American Association of State Highway and Transportation Officials, Washington, DC.